Conformationally Constrained Renin Inhibitory Peptides: Cyclic (3–1)-1-(Carboxymethyl)-L-prolyl-L-phenylalanyl-L-histidinamide as a Conformational Restriction at the P_2-P_4 Tripeptide Portion of the Angiotensinogen Template

Suvit Thaisrivongs,*,† James R. Blinn,‡ Donald T. Pals,† and Steve R. Turner†

Departments of Cardiovascular Diseases Research and Computational Chemistry, Upjohn Laboratories, The Upjohn Company, Kalamazoo, Michigan 49001. *Received June 18, 1990*

Interest in conformationally constrained peptides as potential inhibitors of renin led us to examine an N-terminal cycle of linear renin inhibitory peptides. A cyclic structure was prepared by joining the N-terminal proline at the P_4 site to the imidazole ring of histidine at the P_2 site via a carboxymethylene fragment. An efficient synthetic route to this 14-membered macrocycle was developed and this N-terminal cyclic tripeptide could be readily incorporated into renin inhibitory peptides. Monte Carlo molecular modeling methods were used to generate bound conformations of a representative inhibitor in a model of the renin active site, suggesting possible modes of binding of these inhibitors to renin. Two representative compounds that contain this 14-membered macrocycle were evaluated for their inhibitory activities against human plasma renin and they were found to exhibit very high binding affinity with IC_{50} values in the nanomolar and subnanomolar range.

The renin–angiotensin system has been implicated in several forms of hypertension.[1] Renin catalyzes the first and rate-limiting step of the cascade by cleaving the substrate angiotensin to form the decapeptide angiotensin I. This intermediate is further hydrolyzed by angiotensin converting enzyme to yield the biologically active octapeptide angiotensin II. This octapeptide is one of the most potent vasoconstrictors known and it also stimulates secretion of aldosterone and catecholamine, leading to elevation of blood pressure. The uniquely high enzyme specificity of renin offers the potential of selective pharmacological intervention by compounds designed to be its specific inhibitors.[2] Interest in the blockade of renin then has led to rapid development of potent inhibitors by the design of substrate analogues. The most successful approach has been based on the concept of transition-state analogue of the catalytic mechanism of the aspartyl protease.[3] Modifications at the cleavage site to mimic the tetrahedral species of the peptidic bond has generated compounds with very high inhibitory potency in vitro.[4]

Many renin inhibitors have already been shown to lower blood pressure in renin-dependent models by intravenous administration and also by the oral route.[5] In order to be successful pharmaceutical agents, these compounds have to overcome the major obstacles of low oral absorption and rapid biliary clearance. Efforts to discover inhibitors with longer duration of action and higher oral bioavailability continue to make progress.[6] We have initiated a program with the intention to address the stability of these peptidic compounds against proteolytic degradation[7] to discover compounds with increased duration of action in vivo. We had chosen to examine the peptidic bond between the amino acids at the P_2 and P_3 sites[8] as a likely point of cleavage by proteolytic enzymes. In our previous reports, we have described our work on peptidic backbone modifications[7,9] and on a conformationally constrained dipeptide isostere.[10] The feasibility of orally active renin inhibitory peptides from this approach could be demonstrated.[11] The present study discusses a continuation of our work in this area with compounds that contain a new cyclic structure.

Previous molecular modeling studies have suggested many potential cyclic inhibitors of renin. For statine-containing renin inhibitors, cyclic peptides with N-terminal and C-terminal cycles have been prepared with disulfide bridges.[12] In the template with a reduced bond isostere at the cleavage site, cyclic structures were proposed from the proximity of the side chain at the P_1 site and the main chain NH of the residue at P_2.[13] A series of small cyclic peptides[14] with variable linkers between the N-terminal at P_3 and the side chain at P_2 has been prepared with a glycol function replacing the scissile amide bond. In this report, we describe our work on the N-terminal cycle for the hydroxyethylene-isostere-containing renin inhibitors. During the course of our work on modifications of the N-terminal of renin inhibitory peptides, we observed the formation of an unusual macrocyclic structure at the P_2-P_4 site. The 14-membered ring was formed between the nucleophilic nitrogen atom of proline at P_4 and that of the imidazole ring at P_2 via a two-carbon bifunctional elec-

‡ Computational Chemistry.
† Cardiovascular Diseases Research.

(1) Davis, J. O. *Circ. Res.* **1977**, *40*, 439. Swales, J. D. *Pharmacol. Ther.* **1979**, *7*, 172.
(2) Peach, M. J. *Physiol. Rev.* **1977**, *57*, 313. Ondetti, M. A.; Cushman, D. W. *Annu. Rev. Biochem.* **1982**, *51*, 283. Haber, E. *N. Engl. J. Med.* **1984**, *311*, 1631.
(3) Wolfenden, R. *Transition States of Biochemical Processes*; Gandour, R. D., Schowen, R. L., Eds.; Plenum: New York, 1978; p 555.
(4) Boger, J. *Annu. Rep. Med. Chem.* **1985**, *20*, 257.
(5) Greenlee, W. J. *Pharm. Res.* **1987**, *4*, 364.
(6) Luther, R. R.; Stein, H. H.; Glassman, H. N.; Kleinert, H. D. *Drug. Res.* **1989**, *39*, 1.
(7) Thaisrivongs, S.; Pals, D. T.; Harris, D. W.; Kati, W. M.; Turner, S. R. *J. Med. Chem.* **1986**, *29*, 2088.
(8) Nomenclature as described by Schechter and Berger (*Biochem. Biophys. Res. Commun.* **1967**, *27*, 157), P_n-P_n' refer to the side-chain positions of the peptide substrate.
(9) Thaisrivongs, S.; Pals, D. T.; Harris, D. W.; Kati, W. M.; Turner, S. R. *J. Med. Chem.* **1987**, *30*, 536.
(10) Thaisrivongs, S.; Pals, D. T.; Turner, S. R.; Kroll, L. T. *J. Med. Chem.* **1988**, *31*, 1369.
(11) Pals, D. T.; Thaisrivongs, S.; Lawson, J. A.; Kati, W. M.; Turner, S. R.; Degraaf, G. L.; Harris, D. W.; Johnson, G. A. *Hypertension* **1986**, *8*, 1105.
(12) Boger, J. Renin Inhibitors. Design of Angiotensinogen Transition-State Analogs Containing Statine. Conformationally Restricted Inhibitors and a Model for the Bound Conformation of Renin Substrate. In *Aspartic Proteinases and their Inhibitors*; Walter de Gruyter & Co.: Berlin, Germany, 1985; pp 401–420.
(13) Sham, H. L.; Bolis, G.; Stein, H. H.; Fesik, S. W.; Marcotte, P. A.; Plattner, J. J.; Rempel, C. A.; Greer, J. *J. Med. Chem.* **1988**, *31*, 284.
(14) Sham, H. L.; Rempel, C. A.; Stein, H.; Cohen, J. *J. Chem. Soc., Chem. Commun.* **1990**, 666.

0022-2623/91/1834-1276$02.50/0

Scheme I. Synthesis of the Cyclic Tripeptide 7[a]

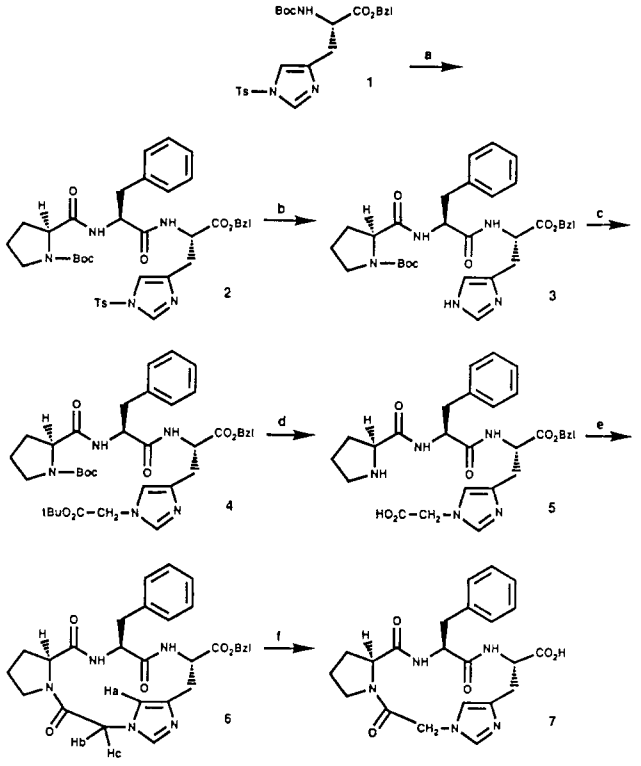

[a] (a) TFA, CH_2Cl_2; Boc-Pro-Phe-OH, $(EtO)_2P(O)CN$, iPr_2NEt, CH_2Cl_2; (b) 1-hydroxybenzotriazole, MeOH; (c) $BrCH_2CO_2tBu$, iPr_2NEt, CH_2Cl_2; (d) TFA; (e) BOP reagent, DMAP, CH_2Cl_2; (f) 5% Pd/C, HCO_2NH_4, DMF.

trophile. We then optimized the synthetic route to this macrocycle and incorporated this cyclic structure into renin inhibitory peptide template. We have also explored the most likely conformers of this ring system by molecular mechanics. This cyclic structure was attached to the remaining peptide template and the mode of binding to the active site of renin was then studied by molecular modeling. We have also searched for plausible binding conformations of the cyclic inhibitor in a model of the renin active site using a Monte Carlo/molecular mechanics search method.

Chemistry

Synthesis of the Cyclic Tripeptide 7. As shown in Scheme I, the synthesis started with the protected histidine **1**. The *tert*-butyloxycarbonyl protecting group was removed with trifluoroacetic acid and the resulting amine was then coupled to *N*-(*tert*-butyloxycarbonyl)-L-prolyl-L-phenylalanine using diethylphosphoryl cyanide[15] to give the protected linear tripeptide **2**. The *p*-toluenesulfonyl group was removed with 1-hydroxybenzotriazole to give compound **3**. Alkylation of the imidazole with *tert*-butyl bromoacetate led to compound **4** in good yield. The alkylation was expected to occur on the τ-nitrogen of the imidazole ring as shown and this assignment was supported by NMR spectroscopic analysis (vide infra). The *tert*-butyloxycarbonyl protecting group and the *tert*-butyl ester were simultaneously removed with trifluoroacetic acid to give amino acid **5**. Lactam ring **6** was then formed under high dilution of the starting material **5** with BOP reagent [benzotriazol-1-yloxytris(dimethylamino)phosphonium hexafluorophosphate][16] and 4-(dimethylamino)pyridine

Scheme II. Synthesis of the Peptides 9 and 12[a]

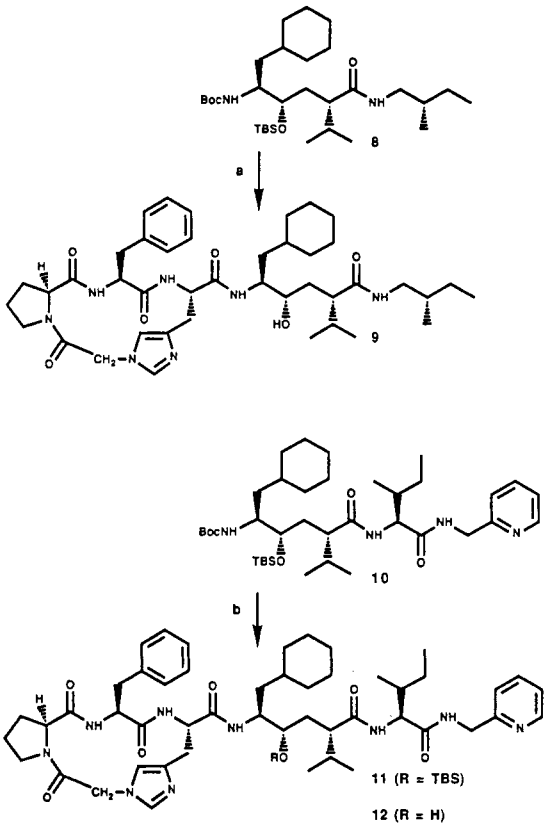

[a] (a) HCl(g), ether; acid **7**, BOP reagent, DMAP, iPr_2NEt, DMF; (b) TFA, CH_2Cl_2; acid **7**, BOP reagent, DMAP, iPr_2NEt, DMF; TFA.

with a yield of 78%. The previous alkylation on the τ-nitrogen of the imidazole ring was supported by ^1H NMR analysis of compound **6**. H_a appeared as a singlet at δ 6.63, whereas H_b and H_c appeared as two doublets at δ 4.58 and 4.7. NOE enhancement could be observed for H_a when H_b and H_c were irradiated. Conversely, NOE enhancement could also be observed for H_b and H_c when H_a was irradiated. The benzyl ester in compound **6** was then hydrogenolyzed to give the building block acid **7**.

Synthesis of the Peptides 9 and 12. As shown in Scheme II, the synthesis of the final peptide **9** started with compound **8**, which was obtained from the coupling of the protected hydroxyethylene isostere building block[17] with 2(*S*)-methylbutylamine. The *tert*-butyloxycarbonyl group and the *tert*-butyldimethylsilyl ether were removed with hydrogen chloride in diethyl ether. The resulting amine hydrochloride was then coupled to acid **7** with BOP reagent to give desired peptide **9**. The synthesis of the final peptide **12** started with compound **10**, which was obtained from the coupling of the protected hydroxyethylene isostere building block[17] with L-isoleucyl-2-pyridylmethylamine. The *tert*-butyloxycarbonyl protecting group was removed with trifluoroacetic acid. The isolated amine was coupled to acid **7** with BOP reagent to give compound **11**. The *tert*-butyldimethylsilyl ether was removed after prolonged treatment of this material with trifluoroacetic acid to give desired peptide **12**.

(15) Yamada, S.; Kasai, Y.; Shioiri, T. *Tetrahedron Lett.* **1973**, 1595.

(16) Castro, B.; Dormay, J. R.; Evin, G.; Selve, C. *Tetrahedron Lett.* **1975**, 1219.

(17) For synthesis of the hydroxyethylene isostere insert, see: Hester, J. B.; Pals, D. T.; Saneii, H. H.; Sawyer, T. K.; Schostarez, H. J.; TenBrink, R. E.; Thaisrivongs, S. European Patent Application, Publication Number 0173481, 1986.

Molecular Modeling Study

The molecular modeling study of human renin–inhibitor interaction was based on a putative structure of human renin–substrate fragment complex as studied by Carlson.[18] The computer-assisted model of human renin was derived from the 3-D coordinates of several fungal aspartyl proteases since X-ray diffraction studies of *Rhizopus chinensis*, *Penicillium janthanellum*, and *Endothia parasitica*, which exhibited varying degrees of sequence homology to human renin, have been determined at a resolution of 1.8–3.0 Å. Recently, it was reported that the root mean square (RMS) difference between the coordinates of the active site residues in a newly determined human renin structure and those of fungal aspartyl proteases was ca. 0.45 Å.[19] For the same set of residues, the RMS difference between that of *R. chinensis*[20] and this computer-assisted human renin model was found to be ca. 0.60 Å. This evidence is taken to support the close approximation of the previously derived human renin model, which was used in this study, to the recently determined coordinates of human renin. The octapeptide substrate fragment His-Pro-Phe-His-Leu-Val-Ile-His of the binary structure in the human renin–substrate complex was derived from the coordinates of pepstatin as bound to the aspatyl protease of *R. chinensis*.[21] A previous modeling study has shown that the structure of a bound substrate-based inhibitor could be constructed from this model of human renin–substrate fragment complex, and that the conformation of this inhibitor is similar to the X-ray structure of the same inhibitor as bound to the *R. chinensis* enzyme.[22]

Interactive molecular modeling was performed with the Mosaic molecular modeling program, which is derived from the MacroModel program.[23] Energy calculations including Monte Carlo searching were performed with the BatchMin program[23] using the AMBER force field[24] as implemented in MacroModel 2.5, with a distance-dependent dielectric ($\epsilon_{ij} = r_{ij}$ in angstroms). Lack of an explicit solvation treatment is a reasonable approximation in this case since the volume of interest (the bound ligand) is highly desolvated.

A simple *N*-methyl amide of the cyclic N-terminal tripeptide was initially modeled in vacuo using systematic[25] or Monte Carlo[26] conformational searching methods. These preliminary results showed that there were a large number of energetically accessible conformations and that a *cis* acetyl-Pro amide bond was allowed in the ring, although not required. However, a program[27] to dock these ring conformers into the renin model in such a way as to allow them to connect to the remainder of the C-terminal fragment discarded most of the structures due to bad steric contacts; consequently the overall sampling efficiency was poor. We therefore turned to Monte Carlo conformational searching of the cyclic tripeptide portion in the active site. As a starting point we used a molecular dynamics average structure[28] for the related linear structure, compound **13** (Ac-Pro-Phe-His-LeuΨ[CH(OH)CH_2]Val-Ile-NH_2). The ligand and all atoms within 7.0 Å were subjected to harmonic restraints; atoms in residues within 3.5 Å of the 7.0-Å shell were included in the energy calculation but were not allowed to move. The structure was subjected to 50 iterations of block diagonal Newton–Raphson minimization at successive restraining potentials of 10.0, 1.0, and 0.0 kcal/mol Å, improving the geometry without large movements overall. For subsequent calculations protein atoms in residues within 10 Å of the cyclized N-terminal tripeptide were included in the energy calculation but were held fixed, as were ligand atoms from the His amide to the C-terminus. An initial cyclized model was constructed by rotation about the Phe ϕ and His χ_1, χ_2 angles, allowing a bond to be formed between the acetyl and the imidazole; the acetyl-Pro amide remained trans. The N-terminal cyclized tripeptide was relaxed (300 iterations) within the fixed active site to give the starting structure for the Monte Carlo search. Monte Carlo searching was performed varying both the Pro and the 14-membered rings, using the linker carbonylmethylene and the Pro γ–δ bonds as the closure bonds. The Pro ϕ, Ψ, and χ_1, Phe ϕ, and His χ_1 and χ_2 bonds were varied explicitly. Bonds adjacent to the closure bonds, including the linker-Pro amide, were varied implicitly as part of the ring closure process. The Monte Carlo run was 1000 steps, usage-directed, with 250 steps of Polak–Ribiere conjugate gradient minimization at each step; structures more than 20.0 kcal/mol above the current lowest energy structure were discarded during the search. Overall this search protocol requires that the ligand bind as similarly as possible to linear compound **13**. The active site geometry is fixed to that for binding the linear ligand and the ligand cannot translate along the active site cleft since the C-terminal portion is fixed. The Pro ω, Phe Ψ, χ, ω, and His ϕ, Ψ, and ω angles are not varied other than incidentally during minimization. Due to these restrictions, as well as the lack of explicit solvation treatment and the static nature of energy minimization, the relative energies will not be particularly accurate, but any ligand conformations found under these restrictive conditions

Table I. Energies of Lowest Energy Members of First Five Clusters

cluster	conformation	energy, kcal/mol
1	1	−60.13
2	4	−55.92
3	9	−53.50
4	11	−52.73
5	24	−51.19

Table II. Energies of Conformation in Cluster 1

conformation	energy, kcal/mol	conformation	energy, kcal/mol
1	−60.13	10	−53.24
2	−59.63	20	−51.83
3	−58.22	34	−49.63
5	−54.75	62	−42.73
8	−53.60		

(18) Carlson, W.; Karplus, M.; Haber, E. *Hypertension* **1985**, *7*, 13.
(19) Sielecki, A. R.; Hayakawa, K.; Fujinaga, M.; Murphy, M. E. P.; Fraser, M.; Muir, A. K.; Carilli, C. T.; Lewicki, J. A.; Baxter, J. D.; James, M. N. G. *Science* **1989**, *243*, 346.
(20) Suguna, K.; Bott, R. R.; Padlan, E. A.; Subramanian, E.; Sheriff, S.; Cohen, G. H.; Davis, D. R. *J. Mol. Biol.* **1987**, *196*, 877.
(21) Bott, R.; Subramian, E.; Davies, D. R. *Biochemistry* **1982**, *21*, 6956.
(22) Sawyer, T. K.; Pals, D. T.; Mao, B.; Maggiora, L. L.; Staples, D. J.; deVaux, A. E.; Schostarez, H. J.; Kinner, J. H.; Smith, C. W. *Tetrahedron* **1988**, *44*, 661.
(23) Mohamadi, F.; Richards, N. G. J.; Guida, W. C.; Liskamp, R.; Lipton, M.; Caufield, C.; Chang, G.; Hendrickson, T.; Still, W. C. *J. Comput. Chem.* **1990**, *11*, 440–467.
(24) Weiner, S. J.; Kollman, P. A.; Case, D. A.; Singh, U. C.; Ghio, C.; Alagona, G.; Profeta, S.; Weiner, P. *J. Am. Chem. Soc.* **1984**, *106*, 765.
(25) Lipton, M.; Still, W. C. *J. Comput. Chem.* **1988**, *9*, 343.
(26) Chang, G.; Guida, W. C.; Still, W. C. *J. Am. Chem. Soc.* **1989**, *111*, 4379.
(27) Blinn, J. R., unpublished results.
(28) Sawyer, T. K.; Mao, B.; Liu, L.; Staples, D. J.; Maggiora, L. L., manuscript in preparation.

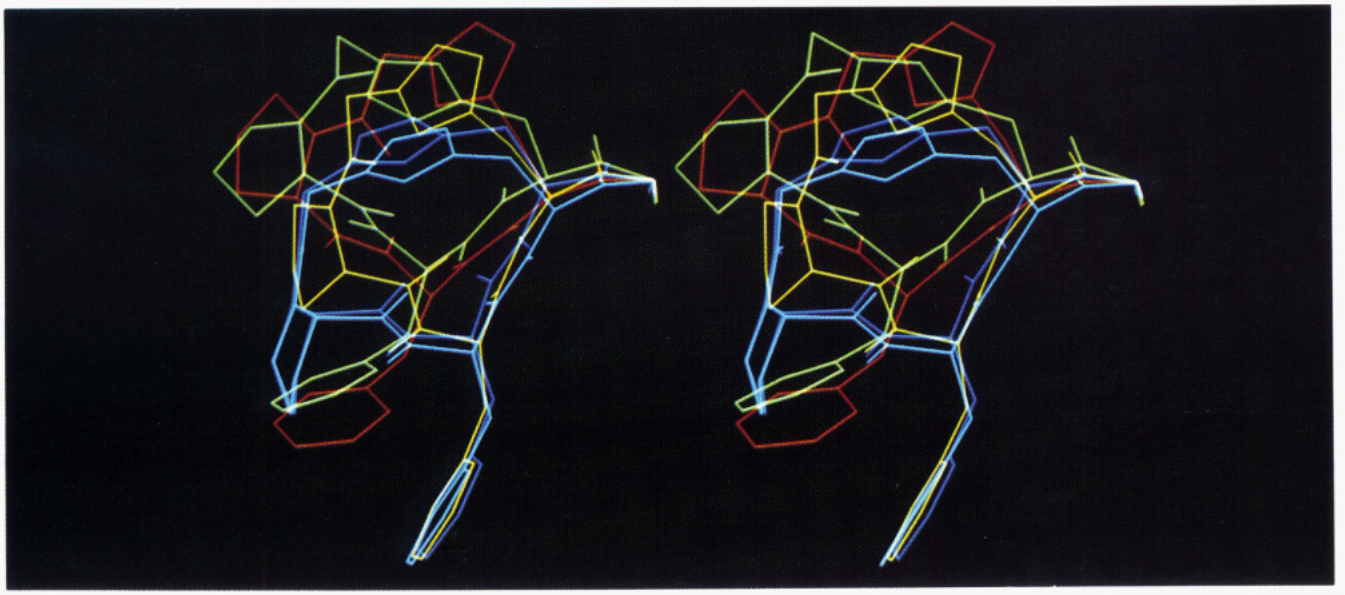

Figure 1. Lowest energy cyclic structure from each of the five clusters. Blue, aqua, green, orange, and red structures correspond to conformations 1, 4, 9, 11, and 24.

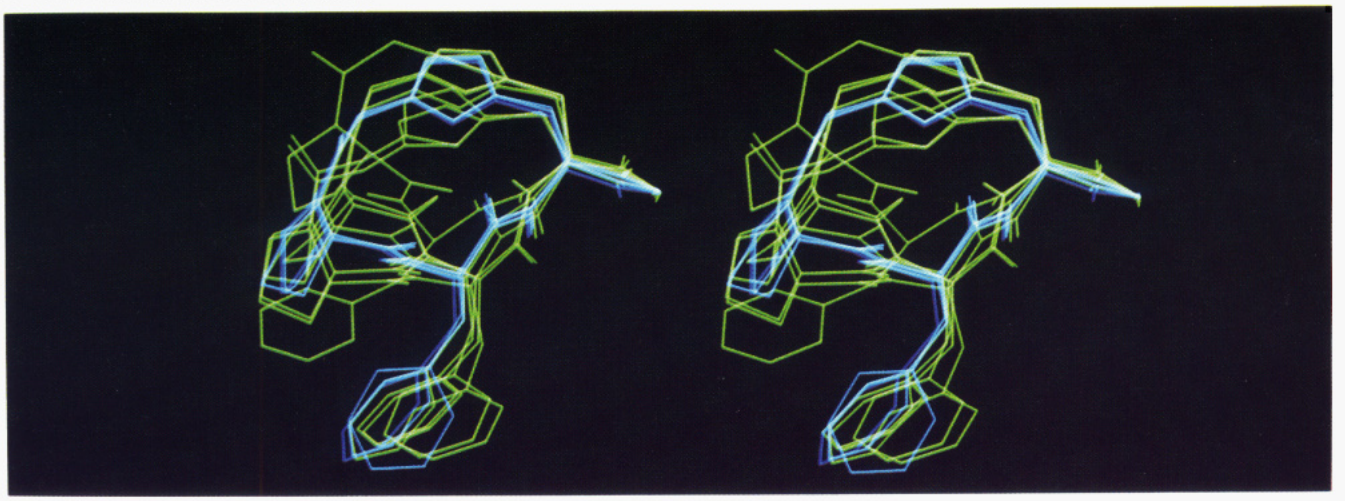

Figure 2. Cyclic structures from the first cluster that contains the overall lowest energy cyclic structure. Conformation 1 is in dark blue; conformations 2 and 3 are in light blue; the remaining six conformations are in green.

should be readily accomodated by the active site in the proper geometry to bind to the enzyme.

In 1000 Monte Carlo steps, 135 structures survived within the 20.0 kcal/mol energy limit; each was found an average of 3.5 times, indicating that the search was reasonably thorough although not exhaustive. The starting structure was 23.4 kcal/mol higher in energy than the best structure found. The structures were further minimized in the fixed active site to an RMS gradient of less than 0.01 kJ/mol Å to give 69 distinct structures after duplicate elimination. The 69 structures found were clustered[29] on the basis of dihedral angles of the 14-membered ring, and five clusters accounted for the 37 lowest energy structures (44 out of 69 structures overall). The first two clusters, which included the eight lowest energy structures, contained structures with a cis amide bond between the linker and the Pro. These two clusters differed primarily in the orientation of the imidazole ring. Although cis peptide bonds are not normally accessible, they are allowed when they precede proline,[30] and *cis*-Xaa-Pro amides have been found in both small cyclic peptides[31] and globular proteins.[32] Structures from the other three clusters, which included all trans amides, formed fewer hydrogen bonds to the active site in this model. Figure 1 shows the overlay of the lowest energy conformation from each of the five clusters. The energies of these structures are shown in Table I.

The position of the phenylalanine side chain in conformations 9 and 24 differs markedly from that of conformations 1, 4, and 11. Figure 2 shows the overlay of the nine structures from the first cluster in order to illustrate the structural variation within a cluster. The energies of these structures are shown in Table II. One conformation shows a very different position for the phenylalanine side chain from the rest of the group. The first three conformations are within 2 kcal/mol in energy, and they are very similar in structure.

The lowest energy cyclic structure (conformation 1), shown in Figure 3, primarily differs from the structure of compound **13** in having a *cis*-linker-Pro amide, a 105°

(29) Moon, J. B., program CLUSTER, unpublished.
(30) Richardson, J. S. *Adv. Protein Chem.* **1981**, *34*, 167.
(31) Karle, I. L.; Karle, J.; Wieland, T.; Bergermeister, W.; Faulstich, H.; Witkop, B. *Proc. Natl. Acad. Sci. U.S.A.* **1973**, *70*, 1836.
(32) Wyckoff, H. W.; Tsernoglou, D.; Hanson, A. W.; Knox, J. R.; Lee, B.; Richards, F. M. *J. Biol. Chem.* **1970**, *245*, 305.

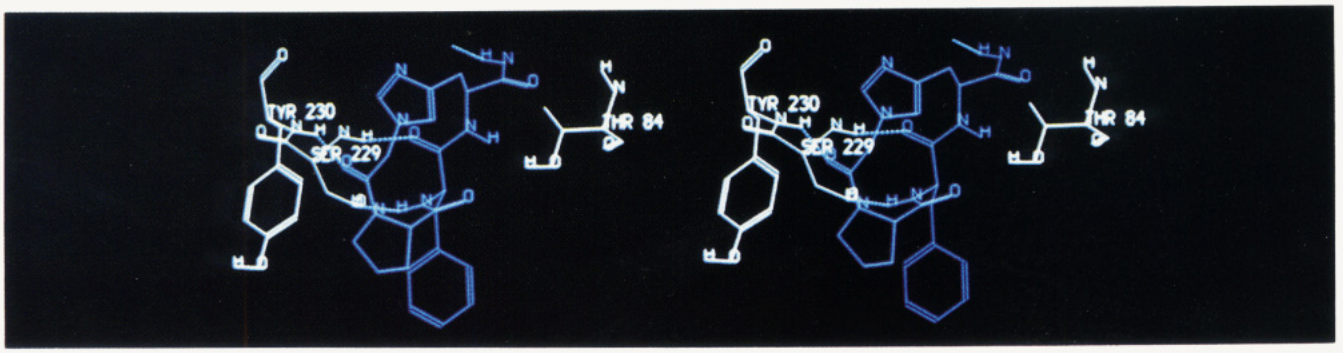

Figure 3. The lowest energy cyclic structure in the active site model. Dashed lines show strong hydrogen bonds.

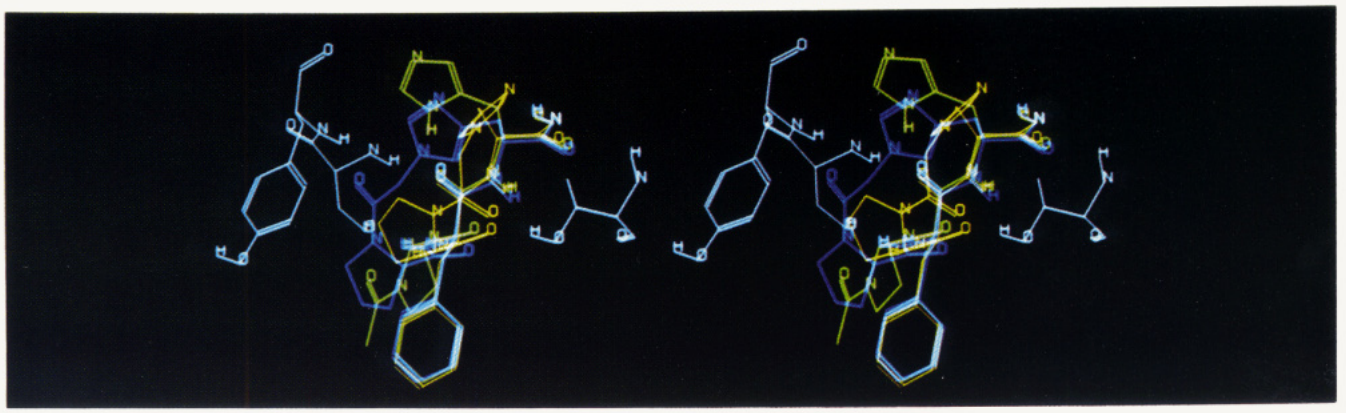

Figure 4. Comparison of binding models. The lowest energy cyclic structure with *cis*-acetyl-Pro linker is shown in blue. The cyclic structure with *trans*-acetyl-Pro linker is shown in orange. The linear structure (compound **13**) is shown in green.

rotation about Pro Ψ, and 126° and 117° rotations about the His χ_1 and χ_2 bonds. As shown in Figure 4, the cyclic structure binds similarly to linear compound **13** in this model; both form hydrogen bonds with the Ser-229 hydroxyl and amide and a weak hydrogen bond with the Thr-84 hydroxyl. Unlike the model for compound **13**, the cyclic structure also makes a strong hydrogen bond between the Tyr-230 amide and the carbonyl of the linker, whereas in compound **13** the corresponding acetyl carbonyl makes an internal C_7 hydrogen bond to the Phe amide which does not contribute to ligand binding. Conformation **11** with the *trans*-linker-Pro amide is shown in orange in Figure 4 for comparison. It is interesting to note that if the model for compound **13** is modified so that the N-terminus is in the same conformation as the cyclic structure (i.e. *cis*-acetyl-Pro amide, 105° rotation about Pro Ψ), the resulting energy-minimized bound conformation is calculated to be 5–7 kcal/mol more stable than the original conformation (5.2 kcal/mol using a solvent-accessible surface area based solvation model[33]). This suggests that in the particular case of compound **13** (i.e. Ac-Pro-...) the *cis*-amide conformation may contribute significantly to binding, although that would not be expected to be the case if the acetyl is replaced by a larger, more hydrophobic group.

Results on Renin Inhibition

Peptides **9** and **12** were tested for their inhibitory activities in vitro against human plasma renin at pH 6. Their IC_{50} values were determined to be 2.2 and 0.28 nM, respectively. The binding affinity compares very favorably with that which is expected of the linear congeners. The linear peptide **13** inhibits human plasma renin with an IC_{50} value of 0.55 nM. Boc-Phe-His-LeuΨ[$CHOHCH_2$]Val-Ile-Amp,[34] which is a closer linear analogue of compound **12**, was found to inhibit renin with an IC_{50} value of 0.36 nM. We are interested in determining the pharmacokinetics property of these cyclic compounds in order to assess potentially improved pharmacological activity in animal model.

Conclusion

In this study, we proposed a cyclic tripeptide structure for the N-terminal P_2-P_4 site of renin inhibitory peptides. The ring structure was formed by a two-carbon bifunctional electrophile connecting the nucleophilic N-terminal proline and the imidazole ring of histidine. The bound conformers for renin inhibitory peptides that contain this N-terminal cycle were also investigated with the molecular model of human renin. The conformation of the bound cyclic structure was found to be closely related to that of the linear reference compound with slight adjustment of the proline and the imidazole rings. The two representative peptides **9** and **12** were readily prepared and their inhibitory activities against human plasma renin was assessed in vitro. Both compounds were found to possess high binding affinity with IC_{50} values in the nanomolar and subnanomolar range. This study should make additional potential renin inhibitors with this cyclic structural feature available for the study of enzyme-bound conformers. Optimization of desirable physical characteristics of this class of compounds for the purpose of addressing the potential improvement of the resulting biological activities in animal models is under current investigation.

Experimental Section

Solvents for chromatography were Burdick & Jackson and used as received. Reagents were from commercial sources and used without further purification unless otherwise noted. Diethyl ether

(33) Hasel, W.; Hendrickson, T. F.; Still, W. C. *Tetrahedron Comput. Methodol.* **1988**, *1*, 103.

(34) TenBrink, R. E.; Pals, D. T.; Harris, D. W.; Johnson, G. A. *J. Med. Chem.* **1988**, *31*, 671.

was Mallinckrodt anhydrous grade. Dichloromethane for reaction solvent was dried over 4A molecular sieves. Dimethylformamide was Aldrich gold-label grade. Diisopropylethylamine was distilled from calcium hydride. Diethylphosphoryl cyanide was distilled before use. Thin-layer chromatography was performed on Merck precoated plates (silica gel 60, F-254). Column chromatography used 70–230 mesh silica gel 60 and, for flash chromatography, 230–400 mesh grade.

Proton nuclear magnetic resonance (^{1}H NMR) spectra were recorded on a Bruker AM-300 (300 MHz) instrument, in deuterated chloroform. Mass spectra were performed by Physical and Analytical Chemistry of the Upjohn Company. High-pressure liquid chromatography was performed on a Perkin-Elmer Series IV liquid chromatograph operating at 1.5 mL/min using a Brownlee RP-18 10 μm column, with UV monitoring by a Kratos Spectroflow 773 detector, at 225 and 254 nm. A Perkin-Elmer LCI-100 integrator was used for peak data. Solvent A is 10% acetonitrile in water with 0.1% trifluoroacetic acid and solvent B is 10% water in acetonitrile with 0.1% trifluoroacetic acid. Solvent system for peptide **9** is 50% solvent A and 50% solvent B. Solvent system for peptide **12** is 10% solvent A and 90% solvent B.

N^{α}-(*tert*-Butyloxycarbonyl)-L-prolyl-L-phenylalanyl-N^{im}-tosyl-L-histidine Benzyl Ester (2). A solution of 1.96 g (3.9 mmol) of N^{α}-(*tert*-butyloxycarbonyl)-N^{im}-tosyl-L-histidine benzyl ester (**1**) in 10 mL of a 1:1 mixture of trifluoroacetic acid and dichloromethane was allowed to stir for 1 h. The mixture was then slowly added to a stirred solution of 5.6 g of $NaHCO_3$ in 50 mL of water. The resulting mixture was extracted with several portions of dichloromethane and the organic phase was then dried (Na_2SO_4). Concentration of the organic phase gave 1.9 g of the free amine.

To a stirred solution of this free amine and 1.42 g (3.9 mmol) of N^{α}-(*tert*-butyloxycarbonyl)-L-prolyl-L-phenylalanine in 10 mL of dichloromethane was added 0.75 mL (4.3 mmol) of diisopropylethylamine, followed by 0.66 mL (4.3 mmol) of diethylphosphoryl cyanide. After stirring for 18 h, the mixture was concentrated and the residue chromatographed on silica gel with 75% ethyl acetate in dichloromethane to give 2.91 g (3.9 mmol, 100%) of N^{α}-(*tert*-butyloxycarbonyl)-L-prolyl-L-phenylalanyl-N^{im}-tosyl-L-histidine benzyl ester (**2**). ^{1}H NMR ($CDCl_3$): δ 1.42 (s, 9 H), 2.41 (s, 3 H), 5.06 (s, 2 H). HRMS: *m/z* 744.3061 (calcd for $C_{39}H_{46}N_5O_8S$, 744.3067).

N^{α}-(*tert*-Butyloxycarbonyl)-L-prolyl-L-phenylalanyl-L-histidine Benzyl Ester (3). A solution of 1.12 g (1.5 mmol) of N^{α}-(*tert*-butyloxycarbonyl)-L-prolyl-L-phenylalanyl-N^{im}-tosyl-L-histidine benzyl ester (**2**) and 0.61 g (4.5 mmol) of 1-hydroxybenzotriazole in 5 mL of methanol was allowed to stir for 18 h. The reaction mixture was then concentrated and the resulting residue was chromatographed on silica gel with 3–5% methanol in dichloromethane to give 0.89 g (1.5 mmol, 100%) of N^{α}-(*tert*-butyloxycarbonyl)-L-prolyl-L-phenylalanyl-L-histidine benzyl ester (**3**). ^{1}H NMR ($CDCl_3$): δ 1.42 (s, 9 H), 5.16 (s, 2 H). HRMS: *m/z* 590.2992 (calcd for $C_{32}H_{40}N_5O_6$, 590.2978).

N^{α}-(*tert*-Butyloxycarbonyl)-L-prolyl-L-phenylalanyl-N^{im}-[(*tert*-butyloxycarbonyl)methyl]-L-histidine Benzyl Ester (4). To a stirred solution of 0.89 g (1.5 mmol) of N^{α}-(*tert*-butyloxycarbonyl)-L-prolyl-L-phenylalanyl-L-histidine benzyl ester (**3**) in 6 mL of dichloromethane was added 0.29 mL (1.7 mmol) of diisopropylethylamine and then 0.24 mL (1.5 mmol) of *tert*-butyl bromoacetate. After stirring for 18 h, the reaction mixture was then concentrated and the resulting residue was chromatographed on silica gel with 4% methanol in dichloromethane to afford 0.755 g (1.07 mmol, 72%) of N^{α}-(*tert*-butyloxycarbonyl)-L-prolyl-L-phenylalanyl-N^{im}-[(*tert*-butyloxycarbonyl)methyl]-L-histidine benzyl ester (**4**). ^{1}H NMR ($CDCl_3$): δ 1.42 (bs, 9 H), 1.47 (s, 9 H), 4.43 (m, 2 H), 5.16 (m, 2 H). HRMS: *m/z* 704.3657 (calcd for $C_{38}H_{50}N_5O_8$, 704.3659).

L-Prolyl-L-phenylalanyl-N^{im}-(carboxymethyl)-L-histidine Benzyl Ester, Trifluoroacetate (5). A solution of 0.755 g (1.07 mmol) of N^{α}-(*tert*-butyloxycarbonyl)-L-prolyl-L-phenylalanyl-N^{im}-[(*tert*-butyloxycarbonyl)methyl]-L-histidine benzyl ester (**4**) in 2.5 mL of trifluoroacetic acid was allowed to stir for 75 min and then diluted with 2.5 mL of dichloromethane. This solution was then added dropwise to a rapidly stirred 180 mL of 1:2 diethyl ether/hexane. The resulting mixture was then centrifuged and decanted. The residue was resuspended in 1:2 diethyl ether/hexane, centrifuged, and then decanted. The remaining solid was then dried to give 0.83 g (1.07 mmol, 100%) of L-prolyl-L-phenylalanyl-N^{im}-(carboxymethyl)-L-histidine benzyl ester, trifluoroacetate (**5**).

L-Histidine Benzyl Ester, L-Prolyl-L-phenylalanyl-1-(carboxymethyl)-, Cyclic (3–1)-Peptide (6). To a stirred suspension of 0.83 g (1.07 mmol) of L-prolyl-L-phenylalanyl-N^{im}-(carboxymethyl)-L-histidine benzyl ester, trifluoroacetate (**5**), in 0.7 L of dichloromethane were added 0.655 g (5.4 mmol) of 4-(dimethylamino)pyridine and 0.95 g (2.1 mmol) of benzotriazol-1-yloxytris(dimethylamino)phosphonium hexafluorophosphate. After 5 days, the reaction mixture was concentrated and the resulting residue was chromatographed on silica gel with 3–7% methanol in dichloromethane to give 0.44 g (0.83 mmol, 78%) of L-histidine benzyl ester, L-prolyl-L-phenylalanyl-1-(carboxymethyl)-, cyclic (3–1)-peptide (**6**). ^{1}H NMR: δ 1.1 (bm, 1 H), 1.6 (bm, 2 H), 2.0 (bm, 1 H), 2.75 (dd, J_1 = 10 Hz, J_2 = 14 Hz, 1 H), 3.29 (dd, J_1 = 4.8 Hz, J_2 = 14 Hz, 1 H), 4.48 (d, *J* = 14 Hz, 1 H), 4.78 (d, *J* = 14 Hz, 1 H), 4.95 (m, 1 H), 5.21 (s, 2 H), 6.64 (s, 1 H), 7.2 (m, 5 H), 7.3 (m, 5 H), 7.59 (s, 1 H). HRMS: *m/z* 530.2434 (calcd for $C_{29}H_{32}N_5O_5$, 530.2403).

L-Histidine, L-Prolyl-L-phenylalanyl-1-(carboxymethyl)-, Cyclic (3–1)-Peptide (7). A mixture of 106 mg (0.20 mmol) of L-histidine benzyl ester, L-prolyl-L-phenylalanyl-1-(carboxymethyl)-, cyclic (3–1)-peptide (**6**), 189 mg (3.0 mmol) of ammonium formate, and 110 mg of 5% palladium on carbon in 2 mL of dimethylformamide was stirred vigorously under argon for 18 h. The reaction mixture was then filtered through Celite with methanol washings. The filtrate was concentrated under reduced pressure to give 90 mg (0.2 mmol, 100%) of L-histidine, L-prolyl-L-phenylalanyl-1-(carboxymethyl)-, cyclic (3–1)-peptide (**7**). ^{1}H NMR: δ 4.47 (dd, J_1 = 9 H, J_2 = 15 Hz, 2 H), 5.05 (d, *J* = 14 Hz, 1 H), 7.76 (s, 1 H), 8.24 (s, 1 H), 8.78 (s, 1 H). HRMS: *m/z* 440.1961 (calcd for $C_{22}H_{26}N_5O_5$, 440.1934).

***N*-[4-(*S*)-[(*tert*-Butyldimethylsilyl)oxy]-5(*S*)-[(*tert*-butyloxycarbonyl)amino]-6-cyclohexyl-2(*S*)-isopropylhexanoyl]-2(*S*)-methylbutylamine (8).** To a stirred solution of 1.5 g (3.09 mmol) of 4(*S*)-[(*tert*-butyldimethylsilyl)oxy]-5-(*S*)-[(*tert*-butyloxycarbonyl)amino]-6-cyclohexyl-2(*S*)-isopropylhexanoic acid, 0.45 mL (3.8 mmol) of 2(*S*)-methylbutylamine, and 0.8 mL (4.6 mmol) of diisopropylethylamine in 12 mL of dichloromethane at 0 °C was added 0.5 mL (3.27 mmol) of diethylphosphoryl cyanide. The resulting mixture was allowed to warm to room temperature and stirred for 3 h. The mixture was then concentrated and the resulting residue chromatographed on silica gel with 10–20% ethyl acetate in hexane to give 1.7 g (3.06 mmol, 99%) of *N*-[4(*S*)-[(*tert*-butyldimethylsilyl)oxy]-5-(*S*)-[(*tert*-butyloxycarbonyl)amino]-6-cyclohexyl-2(*S*)-isopropylhexanoyl]-2(*S*)-methylbutylamine (**8**). ^{1}H NMR ($CDCl_3$): δ 0.83 (s, 3 H), 0.96 (s, 3 H), 0.91 (s, 9 H), 1.44 (s, 9 H), 2.05 (m, 1 H), 2.93 (m, 1 H), 3.21 (m, 1 H), 3.65 (m, 1 H), 3.75 (m, 1 H), 4.51 (d, *J* = 10 Hz, 1 H), 5.74 (m, 1 H). HRMS: *m/z* 555.4551 (calcd for $C_{31}H_{63}N_2O_4Si$, 555.4557).

[1*S*-[1*R,2*R**,4*R**(2*R**)]]-L-Histidine, L-Prolyl-L-phenylalanyl-1-(carboxymethyl)-*N*-[1-(cyclohexylmethyl)-2-hydroxy-5-methyl-4-[[(2-methylbutyl)amino]carbonyl]hexyl]-, Cyclic (3–1)-Peptide (9).** To a stirred solution of 1.7 g (3.06 mmol) of *N*-[4(*S*)-[(*tert*-butyldimethylsilyl)oxy]-5(*S*)-[(*tert*-butyloxycarbonyl)amino]-6-cyclohexyl-2-(*S*)-isopropylhexanoyl]-2(*S*)-methylbutylamine (**8**) in 20 mL of diethyl ether was added hydrogen chloride gas for 15 min. The resulting precipitated mixture was concentrated to give *N*-[5-(*S*)-amino-4(*S*)-hydroxy-6-cyclohexyl-2(*S*)-isopropylhexanoyl]-2(*S*)-methylbutylamine hydrochloride as a white solid (1.15 g, 3.06 mmol).

To a stirred solution of 27.5 mg (0.073 mmol) of *N*-[5(*S*)-amino-4(*S*)-hydroxy-6-cyclohexyl-2(*S*)-isopropylhexanoyl]-2-(*S*)-methylbutylamine hydrochloride, 32 mg (0.073 mmol) of L-histidine, L-prolyl-L-phenylalanyl-1-(carboxymethyl)-, cyclic (3–1)-peptide (**7**), and 2.4 mg (0.02 mmol) of 4-(dimethylamino)pyridine in 0.7 mL of dimethylformamide were added 25 μL (0.14 mmol) of diisopropylethylamine and 39 mg (0.088 mmol) of benzotriazol-1-yloxytris(dimethylamino)phosphonium hexafluorophosphate. After 18 h, the concentrated reaction mixture was chromatographed on silica gel with 3–5% methanol in di-

chloromethane to give 39.1 mg (0.05 mmol, 70%) of [1*S*-[1*R**,2*R**,4*R**(2*R**)]]-L-histidinamide, L-prolyl-L-phenylalanyl-1-(carboxymethyl)-*N*-[1-(cyclohexylmethyl)-2-hydroxy-5-methyl-4-[[(2-methylbutyl)amino]carbonyl]hexyl]-, cyclic (3–1)-peptide (**9**). ^{1}H NMR: δ 0.9 (m, 12 H), 2.1 (bm, 2 H), 3.0 (bm, 6 H), 3.6 (bm, 2 H), 4.0 (bm, 1 H), 4.53 (d, J = 15 Hz, 1 H), 5.07 (d, J = 14 Hz), 6.64 (bs, 1 H), 7.1 (m, 5 H), 7.69 (d, J = 9.4 Hz, 1 H), 7.77 (bs, 1 H). HRMS: m/z 762.4912 (calcd for $C_{42}H_{64}N_7O_6$, 762.4918). HPLC: k' = 12.6.

***N*-[*N*-[4(*S*)-[(*tert*-Butyldimethylsilyl)oxy]-5(*S*)-[(*tert*-butyloxycarbonyl)amino]-6-cyclohexyl-2(*S*)-isopropylhexanoyl]-L-isoleucyl]-2-pyridylmethylamine (10).** To a stirred solution of 4.8 g (10 mmol) of 4(*S*)-[(*tert*-butyldimethylsilyl)oxy]-5(*S*)-[(*tert*-butyloxycarbonyl)amino]-6-cyclohexyl-2(*S*)-isopropylhexanoic acid, 3.0 g (13.56 mmol) of L-isoleucyl-2-pyridylmethylamine, and 2.5 mL (14.3 mmol) of diisopropylethylamine in 40 mL of dichloromethane at 0 °C was added 1.55 mL (10.1 mmol) of diethylphosphoryl cyanide. The resulting mixture was allowed to warm to room temperature and stirred for 16 h. The mixture was then concentrated and the resulting residue chromatographed on silica gel with 50–75% ethyl acetate in hexane to give 6.9 g (10 mmol, 100%) of *N*-[*N*-[4(*S*)-[(*tert*-butyldimethylsilyl)oxy]-5(*S*)-[(*tert*-butyloxycarbonyl)amino]-6-cyclohexyl-2(*S*)-isopropylhexanoyl]-L-isoleucyl]-2-pyridylmethylamine (**10**). ^{1}H NMR ($CDCl_3$): δ 0.11 (s, 3 H), 0.12 (s, 3 H), 0.9 (s, 9 H), 1.42 (s, 9 H), 7.17 (m, 1 H), 7.26 (d, J = 8 Hz, 1 H), 7.6 (m, 1 H), 8.5 (d, J = 5 Hz, 1 H). HRMS: m/z 689.5023 (calcd for $C_{38}H_{69}N_4O_5Si$, 689.5037).

[1*S*-[1*R,2*R**,4*R**(1*R**,2*R**)]]-L-Histidinamide, L-Prolyl-L-phenylalanyl-1-(carboxymethyl)-*N*-[2-[(*tert*-butyldimethylsilyl)oxy]-1-(cyclohexylmethyl)-5-methyl-4-[[[2-methyl-1-[[(2-pyridylmethyl)amino]carbonyl]butyl]amino]carbonyl]hexyl]-, Cyclic (3–1)-Peptide (11).** A solution of 63.2 mg (0.092 mmol) of *N*-[*N*-[4(*S*)-[(*tert*-butyldimethylsilyl)oxy]-5(*S*)-[(*tert*-butyloxycarbonyl)amino]-6-cyclohexyl-2(*S*)-isopropylhexanoyl]-L-isoleucyl]-2-pyridylmethylamine (**10**) in 0.5 mL of 1:1 trifluoroacetic acid/dichloromethane was allowed to stir for 45 min. It was then partitioned between dichloromethane and saturated aqueous $NaHCO_3$. The organic phase was dried (Na_2SO_4) and then concentrated to give 55 mg of *N*-[*N*-[5(*S*)-amino-4(*S*)-[(*tert*-butyldimethylsilyl)oxy]-6-cyclohexyl-2(*S*)-isopropylhexanoyl]-L-isoleucyl]-2-pyridylmethylamine.

To a stirred solution of the above 55 mg (0.092 mmol) of *N*-[*N*-[5(*S*)-amino-4(*S*)-[(*tert*-butyldimethylsilyl)oxy]-6-cyclohexyl-2(*S*)-isopropylhexanoyl]-L-isoleucyl]-2-pyridylmethylamine, 36.6 mg (0.083 mmol) of L-histidine, L-prolyl-L-phenylalanyl-1-(carboxymethyl)-, cyclic (3–1)-peptide (**7**), and 2.4 mg (0.02 mmol) of 4-(dimethylamino)pyridine in 0.8 mL of dimethylformamide were added 15 μL (0.086 mmol) of diisopropylethylamine and 41 mg (0.093 mmol) of benzotriazol-1-yloxytris(dimethylamino)-phosphonium hexafluorophosphate. After 18 h, the concentrated reaction mixture was chromatographed on silica gel with 2–5% methanol in dichloromethane to give 55 mg (0.054 mmol, 65%) of [1*S*-[1*R**,2*R**,4*R**(1*R**,2*R**)]]-L-histidinamide, L-prolyl-L-phenylalanyl-1-(carboxymethyl)-*N*-[2-[(*tert*-butyldimethylsilyl)oxy]-1-(cyclohexylmethyl)-5-methyl-4-[[[2-methyl-1-[[(2-pyridylmethyl)amino]carbonyl]butyl]amino]carbonyl]hexyl]-, cyclic (3–1)-peptide (**11**). ^{1}H NMR: δ 0.06 (s, 3 H), 0.07 (s, 3 H), 0.8 (m), 0.88 (s), 2.15 (m, 1 H), 2.6 (m, 1 H), 2.85 (dd, 1 H), 3.0 (dd, 1 H), 3.2 (m, 1 H), 3.5 (m, 3 H), 4.0 (m, 1 H), 4.5 (m, 6 H), 6.65 (s, 1 H), 7.2 (m, 5 H), 8.48 (d, J = 4.6 Hz, 1 H). HRMS: m/z 1010.623 (calcd for $C_{55}H_{84}N_9O_7Si$, 1010.626).

[1*S*-[1*R,2*R**,4*R**(1*R**,2*R**)]]-L-Histidinamide, L-Prolyl-L-phenylalanyl-1-(carboxymethyl)-*N*-[1-(cyclohexylmethyl)-2-hydroxy-5-methyl-4-[[[2-methyl-1-[[(2-pyridylmethyl)amino]carbonyl]butyl]amino]carbonyl]hexyl]-, Cyclic (3–1)-Peptide (12).** A solution of 52.9 mg (0.052 mmol) of [1*S*-[1*R**,2*R**,4*R**(1*R**,2*R**)]]-L-histidinamide, L-prolyl-L-phenylalanyl-1-(carboxymethyl)-*N*-[2-[(*tert*-butyldimethylsilyl)oxy]-1-(cyclohexylmethyl)-5-methyl-4-[[[2-methyl-1-[[(2-pyridylmethyl)amino]carbonyl]butyl]amino]carbonyl]hexyl]-, cyclic (3–1)-peptide (**11**) in 0.5 mL of trifluoroacetic acid was allowed to stand for 2 h. The mixture was then partitioned between dichloromethane and saturated aqueous $NaHCO_3$. The organic phase was dried ($MgSO_4$) and then concentrated. The resulting residue was chromatographed on silica gel with 3–9% methanol (saturated with ammonia) in dichloromethane to give 36.9 mg (0.041 mmol, 80%) of [1*S*-[1*R**,2*R**,4*R**(1*R**,2*R**)]]-L-histidinamide, L-prolyl-L-phenylalanyl-1-(carboxymethyl)-*N*-[1-(cyclohexylmethyl)-2-hydroxy-5-methyl-4-[[[2-methyl-1-[[(2-pyridylmethyl)amino]carbonyl]butyl]amino]carbonyl]hexyl]-, cyclic (3–1)-peptide (**12**). ^{1}H NMR: δ 0.8 (m, 12 H), 4.0 (m, 1 H), 4.4 (m, 5 H), 4.6 (m, 1 H), 4.9 (m, 3 H), 6.42 (s, 1 H), 7.0 (m), 8.31 (d, 2 H). HRMS: m/z 896.5384 (calcd for $C_{49}H_{70}N_9O_7$, 896.5398). HPLC: k' = 19.9.

Biology. Inhibition of Human Plasma Renin. These peptides were assayed for plasma renin inhibitory activity as follows: lyophilized human plasma with 0.1% EDTA was obtained commercially (New England Nuclear). The angiotensin I generation step utilized 250 μL of plasma, 2.5 μL of phenylmethanesulfonyl fluoride, 25 μL of maleate buffer (pH 6.0), and 10 μL of an appropriate concentration of peptide in a 1% Tween 80 in water vehicle. Incubation was for 90 min at 37 °C. Radioimmunoassay for angiotensin I was carried out with a commercial kit (Clinical Assays). Plasma renin activity values for tubes with peptide were compared to those for control tubes to estimate percent inhibition. The inhibition results were expressed as IC_{50} values, which were obtained by plotting three to four peptide concentrations on semilog graph paper and estimating the concentration producing 50% inhibition.

Acknowledgment. We thank Randy M. Jensen for ^{1}H NMR spectroscopic analysis of compound **6** and we also are grateful to Sally J. Couch for technical assistance.

Registry No. **1**, 132259-57-5; **2**, 132235-82-6; **3**, 132235-83-7; **4**, 132259-58-6; **5**, 132259-60-0; **6**, 132235-84-8; **7**, 132235-85-9; **8**, 124322-05-0; **8**·HCl(*O*,*N*-deprotected), 124322-07-2; **9**, 132235-86-0; **10**, 124322-00-5; **10** (*N*-deprotected), 132235-90-6; **11**, 132235-87-1; **12**, 132235-88-2; H-His(Ts)-OBzl, 132235-89-3; BOC-Pro-Phe-OH, 52071-65-5; $BrCH_2COOBu$-*t*, 5292-43-3; (*S*)-$H_2NCH_2CHMeEt$, 34985-37-0; H-Ile-$NHCH_2$(2-pyridyl), 97920-16-6; 4(*S*)-[(*tert*-butyldimethylsilyl)oxy]-5(*S*)-[(*tert*-butyloxycarbonyl)amino]-6-cyclohexyl-2(*S*)-isopropylhexanoic acid, 123471-30-7; renin, 9015-94-5; angiotensinogen, 11002-13-4.